Journal of Medicinal Chemistry Article

J. Med. Chem. **2010,** *53,* 4989–5001 **4989**
DOI: 10.1021/jm100481d

6-(3,4-Dichlorophenyl)-1-[(Methyloxy)methyl]-3-azabicyclo[4.1.0]heptane: A New Potent and Selective Triple Reuptake Inhibitor

Fabrizio Micheli,*[,†] Paolo Cavanni,[†] Daniele Andreotti,[†] Roberto Arban,[†] Roberto Benedetti,[†] Barbara Bertani,[†] Michela Bettati,[†] Letizia Bettelini,[†] Giorgio Bonanomi,[†] Simone Braggio,[†] Renzo Carletti,[†] Anna Checchia,[†] Mauro Corsi,[†] Elettra Fazzolari,[†] Stefano Fontana,[†] Carla Marchioro,[‡] Emilio Merlo-Pich,[†] Michele Negri,[†] Beatrice Oliosi,[‡] Emiliangelo Ratti,[†] Kevin D. Read,[∥] Maja Roscic,[§] Ilaria Sartori,[†] Simone Spada,[†] Giovanna Tedesco,[‡] Luca Tarsi,[†] Silvia Terreni,[†] Filippo Visentini,[‡] Alessandro Zocchi,[†] Laura Zonzini,[†] and Romano Di Fabio*[,†]

[†]*Neurosciences Centre of Excellence for Drug Discovery, and* [‡]*Molecular Discovery Research, GlaxoSmithKline Medicines Research Centre, Via Fleming 4, 37135 Verona, Italy,* [§]*GlaxoSmithKline Research Centre Zagreb Ltd., Prilaz Baruna Filipovica 29, 10000 Zagreb, Croatia, and* [∥]*Biological Chemistry and Drug Discovery, College of Life Sciences, Sir James Black Centre, University of Dundee, Dundee, DD1 5EH, Scotland, U.K.*

Received April 20, 2010

A pharmacophore model for triple reuptake inhibitors and the new class of 1-(aryl)-6-[alkoxyalkyl]-3-azabicyclo[3.1.0]hexanes were recently reported. Further investigation in this area led to the identification of a new series of potent and selective triple reuptake inhibitors endowed with good developability characteristics. Excellent bioavailability and brain penetration are associated with this series of 6-(3,4-dichlorophenyl)-1-[(methyloxy)methyl]-3-azabicyclo[4.1.0]heptanes together with high in vitro potency and selectivity at SERT, NET, and DAT. In vivo microdialysis experiments in different animal models and receptor occupancy studies in rat confirmed that derivative **17** showed an appropriate profile to guarantee further progression of the compound.

Introduction

Unipolar depression is a terrible illness characterized by low mood, low self-esteem, and loss of interest or pleasure in usually enjoyable activities. Various drugs have been used for decades to treat depressed patients. In particular, chemicals able to interfere with either the uptake or with the metabolism of aminergic neurotransmitters have found substantial application. Monoamine oxidase (MAO) inhibitors and tricyclic antidepressants achieved large diffusion in the early days, but unfortunately they are associated with some side effects that may hamper their efficacy.[1] In recent times, drugs that selectively block neurotransmitter reuptake in either serotoninergic neurons (SSRI, e.g., paroxetine, Figure 1) or noradrenergic neurons (SNRI, e.g., reboxetine, Figure 1) became the "gold standard" therapies. Additionally, drugs blocking reuptake at both the serotoninergic and the noradrenergic transporters (e.g., venlafaxine, Figure 1) or at both the noradrenergic and the dopaminergic neurons (e.g., bupropion, Figure 1) also demonstrated clinical efficacy and acceptable tolerability;[1] these structures are also referred to as "dual" reuptake inhibitors.

Quite recently, the structures of new compounds that are "triple" reuptake inhibitors[2] (TRUI) were disclosed; some of these, such as indatraline, SEP-225289, and DOV derivatives are reported in Figure 1. The theory on the efficacy of such molecules able to inhibit amine reuptake of the 5-HT, NE, and DA transporters at the same time comes from both preclinical and clinical studies.[3] The concurrent blockade of the uptake of the three aminergic neurotransmitters, and therefore the increased DA levels with respect to the "dual" drugs, might address the anhedonic component of unipolar depression as well as the shortening of the time to onset of clinical efficacy. We have recently reported[3,4] the rational design of two new classes of TRUI endowed with excellent potency and in vivo activity. The use of a TRUI pharmacophore model (Figure 2, left panel) was imperative during medicinal chemistry exploration to appropriately address these three targets simultaneously. In particular, it was crucial in achieving the desired, balanced ratio among the three transporters. In fact, as previously reported,[3] many of the disclosed TRUI show similar levels of inhibition at the three monoamine transporters (SERT[a] ∼ NET ∼ DAT), while our target was to identify molecules with an alternative profile such that SERT ≥ NET > DAT. The key characteristics of this model are represented by the following features: a positive ionizable region, three hydrophobic areas, a region in which an aromatic ring may sit, and an H-bond acceptor zone. As previously described, the

*To whom correspondence should be addressed. For F.M.: phone, +39-045-8218515; fax, +39-045-8118196; e-mail, Fabrizio.E.Micheli@gsk.com. For R.D.F.: phone, +39-045-8218879; fax, +39-045-8118196; e-mail, Romano.M.Di-Fabio@gsk.com.

[a] Abbreviations: hERG, human ether-a go-go related gene K^+ channel; NCE, new chemical entity; PK, pharmacokinetic; P450, cytochrome P450; hCli, human intrinsic clearance; *F*, bioavailability; B/B, brain/blood ratio; Clb, blood clearance; V_d, distribution volume; SPA, scintillation proximity assay; 5-HT, serotonin; NE, norepinephrine or noradrenaline; DA, dopamine; SERT, serotonin transporter; NET, noradrenaline transporter; DAT, dopamine transporter; MD, microdialysis; pK_i, inhibition constant from binding assays; fpK_i, functional inhibition constant for an antagonist from functional assays, e.g., functional inhibition constant obtained from functional inhibition assays using the Cheng−Prusoff equation.

Published on Web 06/09/2010

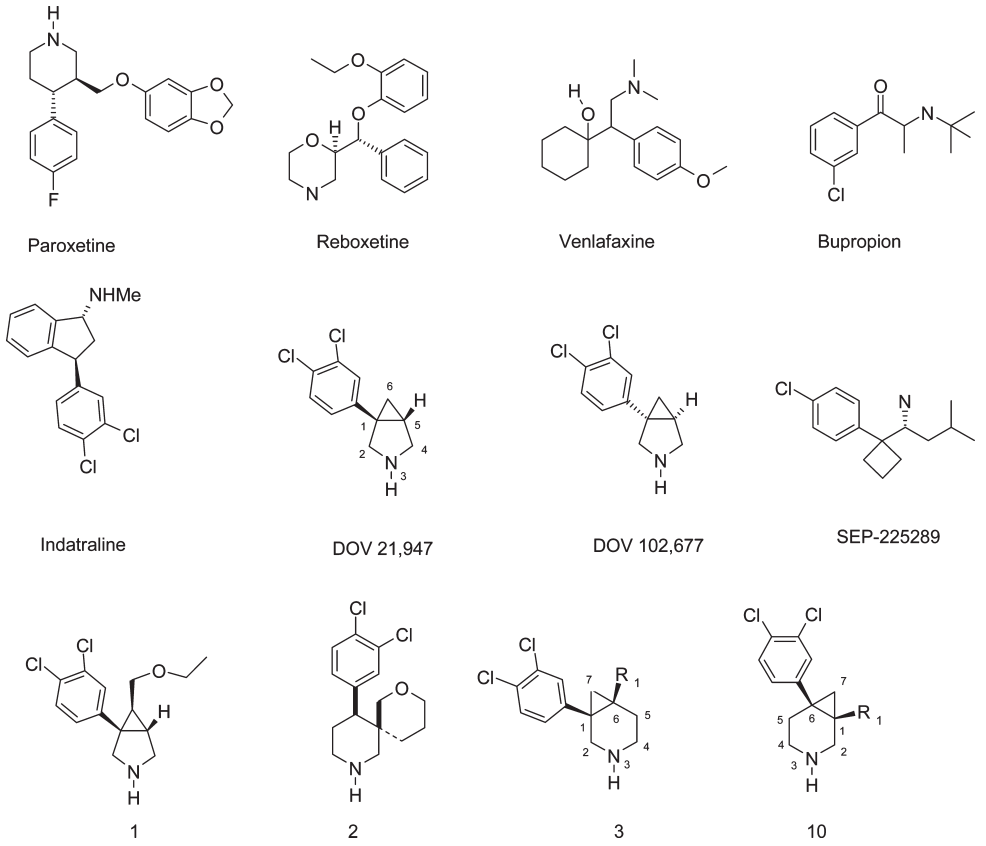

Figure 1. Structures of known monoaminergic reuptake inhibitors.

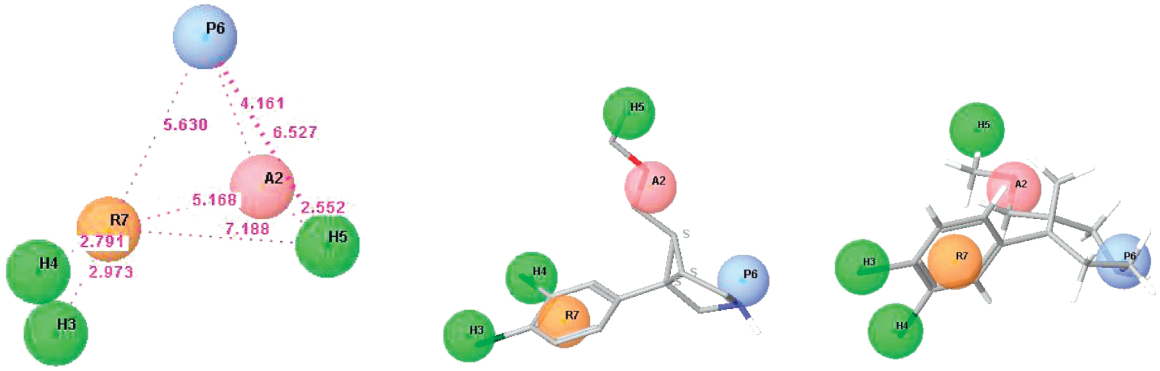

Figure 2. Left: Triple reuptake inhibitors pharmacophore. Coding of features are as follows: blue sphere, positive ionizable; pink spheres, H-bond acceptor; green spheres, hydrophobic; orange sphere, aromatic ring. Distances among the pharmacophoric points are shown in angstroms. Middle: Derivative **1** fitted in the pharmacophore model. Right: Derivative **17** fitted in the pharmacophore model.

presence of a secondary/tertiary amine in the scaffold is fundamental for achieving the primary activity at the three transporters, while the decoration of the aromatic region (hydrophobic areas) provides an appropriate "titration" of the SERT/NET/DAT components. Finally, as will be further exemplified below, the role of the H-bond acceptor in this specific model seems to be critical in determining the DAT affinity.

Results and Discussion

Given the optimal fitting of **1** in the pharmacophore model (Figure 2, middle panel), it was decided to identify alternative bicyclic templates that maintained similar distances between the key points of interaction, namely, the basic nitrogen, the aromatic system, and the side chain. For this reason, the regioisomeric products 1-phenyl-3-azabicyclo[4.1.0]heptane (**3**) and 6-phenyl-3-azabicyclo[4.1.0]heptane (**10**) were synthesized exploiting the Beckmann rearrangement of the 1-phenylbicyclo[3.1.0]hexan-3-one oxime prepared from the corresponding ketone in analogy to literature reports.[5] The enantiomers were separated by chiral HPLC, and the results of their biological evaluation are reported in Tables 1 and 2. It was quite evident that, also on these nonsubstituted [4.1.0]-heptane scaffolds, despite the lack of interaction with one of the key pharmacophoric features in the model, interesting pK_i values could be achieved at the three transporters and that the 6-phenyl-3-azabicyclo[4.1.0]heptane template **10** was slightly superior to the regioisomeric 1-phenyl scaffold **3**. The introduction of an appropriate side chain was the next step in the process. Suitable synthetic schemes were devised to regioselectively place

Table 1. Binding at the Three Transporters (SERT, NET, DAT) Expressed as pK_i [a]

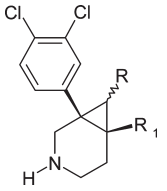

entry	stereochemistry	R_1	R	hSERT SPA pK_i	hNET SPA pK_i	hDAT SPA pK_i
DOV 21,947	NA	NA	NA	6.85	6.83	7.10
DOV 102,677	NA	NA	NA	7.08	7.23	7.42
1	NA	NA	NA	9.80	9.30	8.10
2	NA	NA	NA	9.50	8.40	7.90
3	rac	H	H	6.90	6.80	7.10
4	se	H	H	7.10	7.20	7.40
5	se	H	H	6.60	6.40	7.00
6	rac	CH_2OMe	H	7.50	6.70	6.90
7	se	CH_2OMe	H	6.80	6.00	6.20
8	se	CH_2OMe	H	7.90	7.00	7.20
9	exo (rac)	H	CH_2OMe	7.50	7.20	6.90

[a] Only relative stereochemistry is shown. SEM for hSERT/NET/DAT data sets is ±0.1. rac = racemate. se = single enantiomer. NA = not applicable.

Table 2. Binding at the Three Transporters (SERT, NET, DAT) Expressed as pK_i [a]

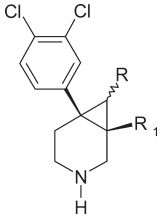

entry	stereochemistry	R_1	R	hSERT SPA pK_i	hNET SPA pK_i	hDAT SPA pK_i
10	rac	H	H	7.60	6.60	7.30
11	se	H	H	7.40	6.60	7.30
12	se	H	H	7.90	7.00	7.60
13	rac	CH_2OH	H	7.70	6.80	6.70
14	se	CH_2OH	H	7.40	6.40	7.00
15	se	CH_2OH	H	8.10	7.00	7.10
16	rac	CH_2OMe	H	8.80	7.90	7.60
17	se	CH_2OMe	H	9.20	8.10	8.00
18	se	CH_2OMe	H	7.70	6.90	7.00
19	endo (rac)	H	CH_2OMe	7.30	5.70	5.90
20	exo (rac)	H	CH_2OMe	8.00	6.50	6.40

[a] Only relative stereochemistry is shown. SEM for hSERT/NET/DAT data sets is ±0.1. rac = racemate. se = single enantiomer.

the alkyl alkoxy side chain in different positions on the new scaffolds. Two of these pathways, illustrated for scaffold **10**, are reported in Schemes 1 and 2, while other specific schemes for this template or for the regioisomeric scaffold **3** are reported in the patent literature.[6,7] The results of this exploration are described in Tables 1 and 2. As predicted by the pharmacophore model, the introduction of the methoxymethyl side chain on derivative **3** in positions 6 (derivatives **6**−**8**) and 7 (derivative **9**) determined a substantial improvement of affinity at the three transporters, with **6** being equipotent to **9** at SERT. Because of synthetic difficulties, only the exo derivative of this latter compound could be tested. The introduction of the same side chain on the regioisomeric template **10** (derivatives **16**−**20**) showed a significant difference between the two branching positions on the scaffold. The introduction in position 1 (derivative **16**) determined an approximately 10-fold increase in affinity for the three transporters with respect to the best results achieved with the side chain in position 7 (exo derivative **20**). Furthermore, a significant difference between the endo and exo isomer (**19** and **20**, respectively) was also noticed, with the latter being about 10-fold more potent than the former on the three human transporters. Derivative **16** was separated by chiral HPLC into its enantiomers (**17**, **18**), and derivative **17** proved to have nanomolar affinity at SERT and excellent affinity at NET and DAT. As previously described,[3] to ensure that appropriate developability characteristics were present in the new scaffolds since the inception of the exploration, generic developability screens such as CYPEX bactosome P450 inhibition and rat and human in vitro clearance in liver microsomes were added early in the biological screening cascade. Also in this case, the methoxymethyl side chain proved to be a stable group. The IC_{50} values for all major P450 isoforms tested (CYP1A2, CYP2C9, CYP2C19, CYP2D6, and CYP3A4) were greater than 10 μM with the exception of CYP2D6 (3 μM), and intrinsic

Scheme 1. General Synthetic Procedures[a]

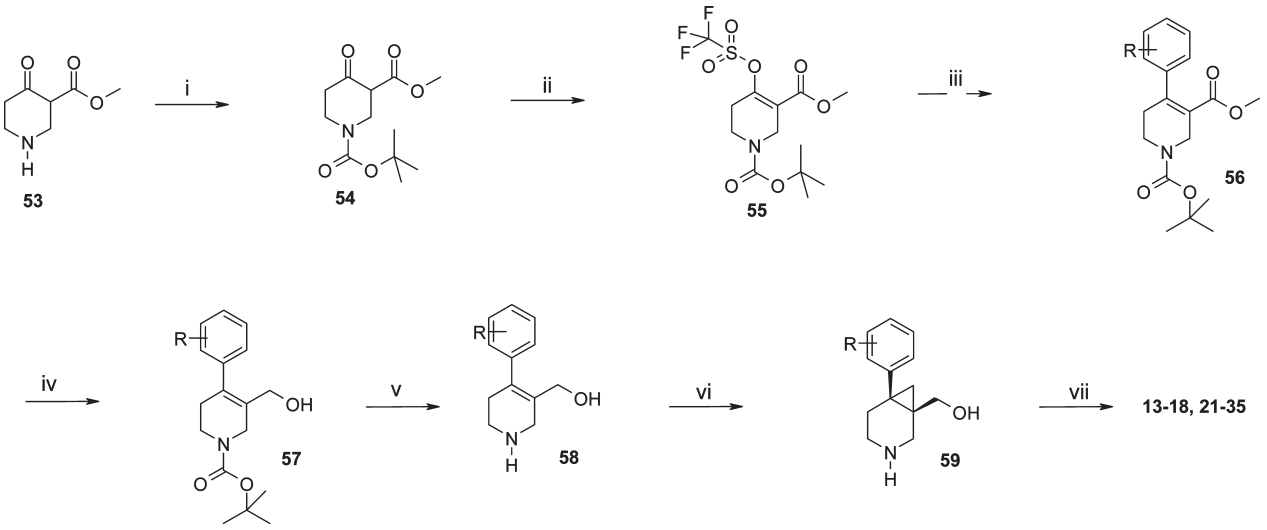

[a] (i) BOC_2O, TEA, CH_2Cl_2, from 0 °C to room temp, 4 h; (ii) (a) NaH, DMF, 0 °C; (b) $PhN(SO_2CF_3)_2$, DMF, room temp; (iii) $ArB(OH)_2$, Na_2CO_3, $Pd(PPh_3)_4$, toluene/EtOH; (iv) $LiAlH_4$ in Et_2O (1 M), −20 °C; (v) TFA, CH_2Cl_2, 0 °C; (vi) CH_2I_2, $ZnEt_2$, CH_2Cl_2; (vi) (a) NaH, DMF, 0 °C; (b) RX, DMF, room temp.

Scheme 2. General Synthetic Procedures[a]

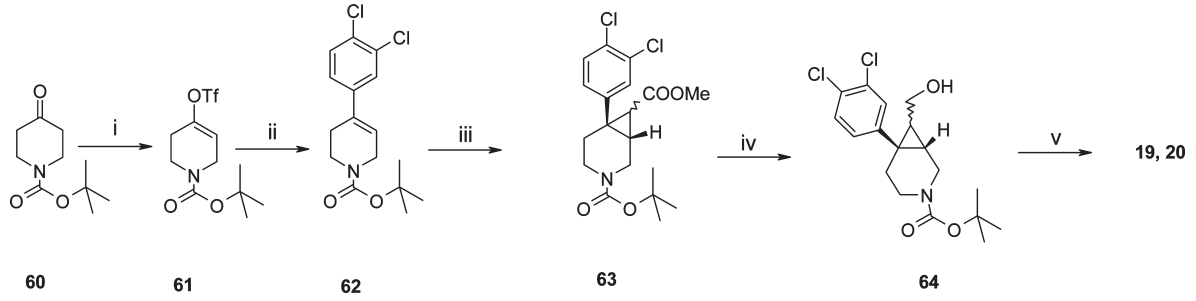

[a] (i) (a) NaH, DMF, 0 °C; (b) $PhN(SO_2CF_3)_2$, DMF, room temp; (ii) 3,4-dichlorophenyl-$B(OH)_2$, Na_2CO_3, $Pd(PPh_3)_4$, toluene/EtOH; (iii) N_2CH_2COOMe, $Rh_2(OAc)_4$, CH_2Cl_2, 60 °C; (iv) $LiAlH_4$ in Et_2O (1 M), −20 °C; (v) (a) NaH, DMF, 0 °C; (b) RX, DMF, room temp; (c) TFA, CH_2Cl_2, 0 °C.

clearance (Cli) values both in human and in rat were moderate (1.4 and 1.8 (mL/min)/g of protein). Interestingly enough, the removal of the methoxy group led to compounds (**13**−**15**) with good affinity at the three transporters. Derivative **15**, in particular, showed a profile superior to the nondecorated template, suggesting that the hydrophilic moiety was well tolerated. Given this premise, it was decided to further explore the role of the side chain and the pattern of substitution of the aromatic ring. Results are reported in Table 3. The presence of a single chlorine atom in position 4 of the phenyl group (**21**) led to a 10-fold decrease of affinity vs SERT/NET/DAT, while the introduction in the same position of a trifluoromethoxy group (**22**) with its slightly larger volume and its lack of mesomeric effect led to the identification of a selective SSRI. Another similar profile with 100-fold selectivity over NET and DAT was achieved by compound **23**, while the replacement of a single chlorine atom with a trifluoromethyl group (**24**, **25**) gave a profile similar to that of the monochloro derivative **21**. Considering the overall dimensions of a $-CF_3$ group, these results might be interpreted, once again, as a consequence of the lack of the retrodonating mesomeric effect. The introduction of a 2-naphthyl substituent (**26**) determined a substantial increase in SERT affinity with respect to derivative **16**, while the effect on NET and DAT was comparable. The pure enantiomer **28** showed a subnanomolar affinity at SERT and low nanomolar affinity at NET and DAT, making this compound extremely interesting for further characterization. The IC_{50} values for all major P450 isoforms tested were greater than 8 μM; the Cli value in human was moderate (1.2 (mL/min)/g of protein), while the Cli value in rat suffered from the nonsubstituted nature of the naphthyl ring (17 (mL/min)/g of protein), suggesting that an appropriate decoration/protection of the group would be necessary before proceeding to preclinical testing in vivo. As far as the exploration of the side chain is concerned, a limited number of examples are reported in Table 3. The introduction of a further methylene (**29**) to the methoxymethyl group led to a superimposable in vitro affinity profile, both as a racemate and as single enantiomers. The replacement of the methyl group with the electron-withdrawing $-CF_3$ moiety (**32**) caused a slight decrease in affinity at the three targets, while the introduction of a cyclopropyl methyl substituent (**33**−**35**) determined a variation in the primary in vitro profile. In fact, derivative **34**, when compared to **17**, showed a more "dual" SERT/DAT profile, making this compound an interesting tool for further exploring the role of a differently balanced reuptake inhibitor.

To probe the role of the ethereal oxygen in the new template, a series of superior H-bond acceptors were prepared; the results are reported in Table 4. The introduction of the ethyl ester in **36** caused a slight increase in NET affinity, a more substantial increase in DAT affinity, and a 10-fold

Table 3. Binding at the Three Transporters (SERT, NET, DAT) Expressed as pK_i [a]

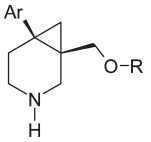

entry	stereochemistry	Ar	R	hSERT SPA pK_i	hNET SPA pK_i	hDAT SPA pK_i
21	rac	4-Cl Ph	Me	7.80	6.70	6.60
22	rac	4-OCF_3 Ph	Me	8.50	5.50	5.10
23	rac	4-F, 3-Cl Ph	Me	8.80	6.50	6.80
24	rac	4-Cl, 3-CF_3 Ph	Me	7.80	6.70	5.50
25	rac	4-CF_3, 3-Cl Ph	Me	7.80	6.90	5.80
26	rac	2-naphthyl	Me	9.50	7.90	7.50
27	se	2-naphthyl	Me	9.00	7.40	7.00
28	se	2-naphthyl	Me	9.90	8.00	7.90
29	rac	3,4- dichloro Ph	Et	8.90	8.00	8.20
30	se	3,4- dichloro Ph	Et	8.00	7.00	7.20
31	se	3,4- dichloro Ph	Et	9.00	8.10	8.40
32	rac	3,4- diChloro Ph	CH_2CF_3	8.20	7.10	7.40
33	rac	3,4- dichloro Ph	CH_2cPr	8.90	7.30	7.90
34	se	3,4- dichloro Ph	CH_2cPr	9.40	7.70	8.50
35	se	3,4- dichloro Ph	CH_2cPr	8.40	6.90	7.20

[a] SEM for hSERT/NET/DAT data sets is ±0.1. Only relative stereochemistry is shown. rac = racemate. se = single enantiomer.

Table 4. Binding at the Three Transporters (SERT, NET, DAT) Expressed as pK_i [a]

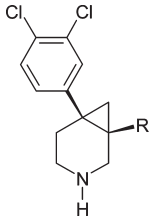

entry	stereochemistry	R	hSERT SPA pK_i	hNET SPA pK_i	hDAT SPA pK_i
36	rac	COOEt	7.80	8.10	8.30
37	rac	$CONH_2$	7.00	6.10	6.60
38	rac	$CONHC_3H_3$	7.00	6.30	6.80
39	se	$COCH_3$	9.00	7.80	8.40

[a] Only relative stereochemistry is shown. SEM for hSERT/NET/DAT data sets is ±0.1. rac = racemate. se = Only one single enantiomer was pure enough for testing.

decrease in the SERT activity, while the more hydrophilic primary amide **37** showed a general decrease at all three targets. This profile did not change with the introduction a lipophilic substituent (**38**), suggesting that the presence of an H-bond donor (NH) in this region might be poorly tolerated; alternatively, it might be hypothesized that a conformational change is caused by the presence of the amide bond and that the potential H-bond acceptor is no longer able to properly act because it is spatially directed elsewhere. The introduction of the methyl ketone **39** (only one enantiomer was tested because neither the racemate nor the other enantiomer could be isolated pure enough for primary testing) led to a profile similar to that of **16** but with a higher DAT component. Accordingly, in agreement with what was previously reported,[3] it might be hypothesized that the potential H-bond acceptor region mapped by the pharmacophore model has lower importance for the SERT and NET transporters, while it might have a greater role in determining the DAT affinity.

The next step in the exploration was related to the investigation of the substitution tolerated by the scaffold and its influence on the role of the nitrogen. These results are reported in Table 5. A small hindrance (Me, **40**) α to the nitrogen (position 4) was well tolerated, with a slight decrease in affinity at the three targets. The introduction of a small electron-withdrawing group β to the nitrogen and therefore theoretically able to change its basicity was then tested. Both stereoisomers of the 5-fluoro derivative (**41**, **42**) demonstrated the same profile at SERT/NET/DAT; considering that, in theory, at least one of the two should have been able to interact with the antibonding orbitals of the C−N bond to influence its basicity, it might be possible to conclude that no major influence of this parameter was observed. On the other hand, the introduction of a methoxy group (**43**, **44**) demonstrated a major influence on the primary in vitro affinity profile at the three transporters. Considering the lower electronegativity of the oxygen atom, it might be reasonable to conclude that this effect was probably more linked to an overall steric effect of the substituent in position 5 rather than to its effect on the overall basicity of the system. Finally, the introduction of a further substituent on the methoxymethyl side chain had a positive effect on the primary in vitro profile of the compounds (**45**, **46**). Both derivatives showed a nanomolar profile at the three targets; in particular **45** demonstrated a subnanomolar profile at SERT and, despite the presence of an allyl group, the IC_{50} values for all major P450 isoforms tested were greater than 3 μM.

The final part of this preliminary exploration on this new template was related to the understanding of the substitution of the nitrogen atom itself. The results are reported in Table 6. The introduction of a methyl group (**47**) caused a decrease in affinity at SERT and NET of about 10-fold and 50-fold, respectively, while almost no effect was observed on DAT affinity. The introduction of a bulkier system (*i*-Pr, **48**) had a profound effect at the three transporters with a strong reduction of affinity. We postulated that this was potentially due to the hindrance of the Me and *i*-Pr groups and not related to the presence of a tertiary nitrogen in the scaffold. To prove this working hypothesis, we set up an appropriate synthetic strategy to prepare a further cyclized scaffold (a 6-azatricyclo[4.2.1.$0^{1,3}$]nonane template).

Table 5. Binding at the Three Transporters (SERT, NET, DAT) Expressed as pK_i [a]

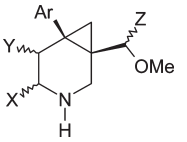

Entry	Stereo.	X	Y	Z	hSERT SPA pKi	hNET SPA pKi	hDAT SPA pKi
40	(rac.)	Me—	H	H	8.10	7.30	7.40
41	(rac.)	H	F····	H	8.30	7.00	7.00
42	(rac.)	H	F—	H	8.40	7.30	7.00
43	(rac.)	H	MeO····	H	7.00	5.90	6.30
44	(rac.)	H	MeO—	H	6.60	5.80	6.40
45*	(rac.)	H	H	Allyl	9.90	9.00	8.90
46**	(rac.)	H	H	Allyl	8.90	8.40	8.80

[a] SEM for hSERT/NET/DAT data sets is ±0.1. Only relative stereochemistry is shown. Stereo. = stereochemistry. rac. = racemate. * = diastereoisomer 1. ** = diastereoisomer 2.

Table 6. Binding at the Three Transporters (SERT, NET, DAT) Expressed as pK_i [a]

Entry	Stereo.	X	hSERT SPA pKi	hNET SPA pKi	hDAT SPA pKi
47	(s.e.)	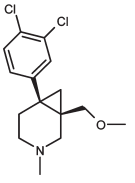	7.90	6.10	7.50
48	(s.e.)	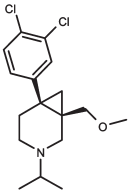	6.20	5.30	5.90
49	(s.e.)	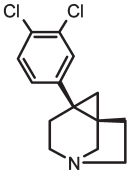	8.80	7.20	7.10
50	(s.e.)	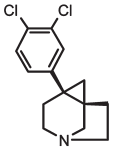	7.50	6.10	6.60

[a] SEM for hSERT/NET/DAT data sets is ±0.1. Only relative stereochemistry is shown. Stereo. = stereochemistry. s.e. = single enantiomer.

As evident from the two separate enantiomers (**49**, **50**), good levels of potency were achieved on the nondecorated scaffold. Further investments are being made to appropriately decorate this new promising scaffold.

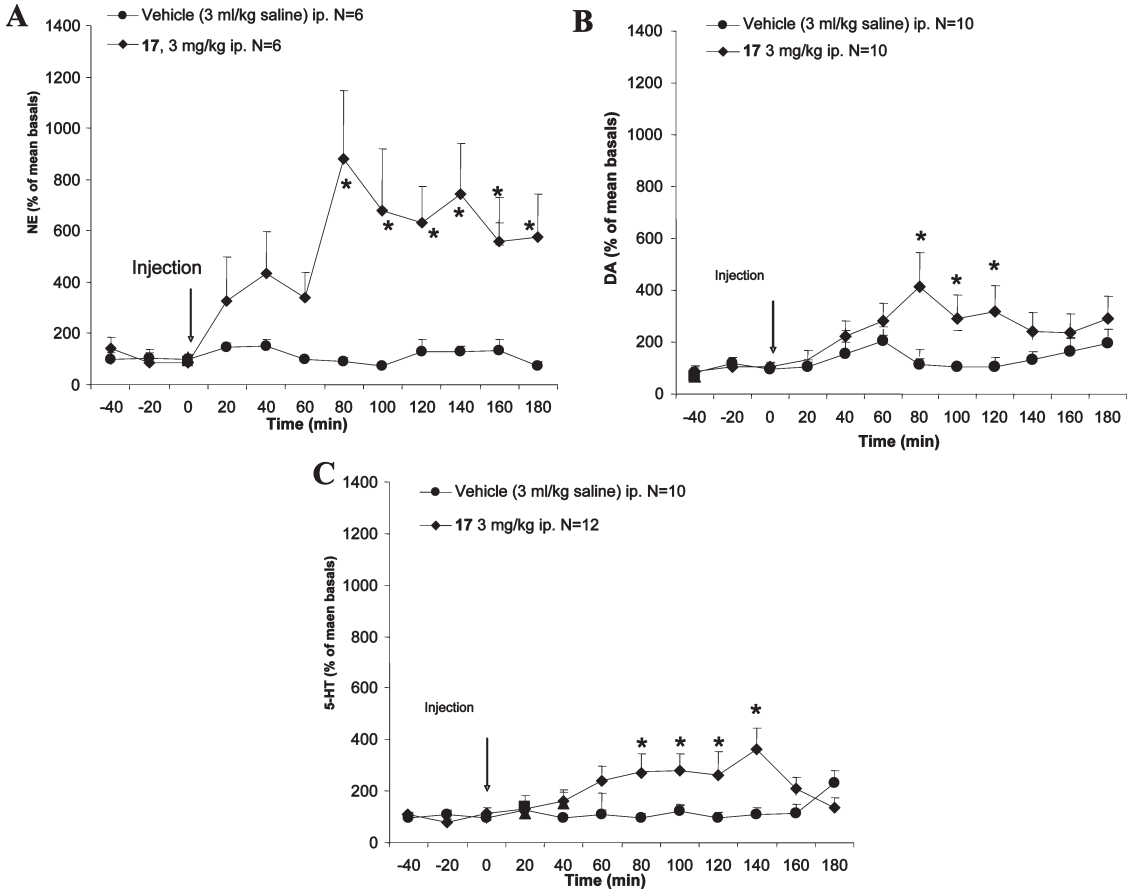

Figure 3. Time course of the effect of **17** (3 mg/kg, ip) on norepinephrine (A), dopamine (B), and serotonin (C) outflow in the rat medial prefrontal cortex. Arrow shows injection, and asterisk (∗) highlights significant difference vs respective vehicle time point (ANOVA with repeated measure of time followed, when appropriate, by planned comparison). Data are the mean ± SEM of neurotransmitter concentration expressed as percentage of basal values.

Further Characterization of Compound 17. The stereochemistry of this molecule was assigned using vibrational circular dichroism (VCD) as previously reported,[3] and derivative **17** was identified as the (1*S*,6*R*) isomer in accordance to the method. This result was subsequently confirmed by X-ray experiments which will be reported in due course.

Subsequently, derivative **17** was tested using filtration assay binding conditions, and the values obtained were in good agreement with the SPA binding ($pK_i = 8.98 \pm 0.02$ ($n = 5$), 7.92 ± 0.02 ($n = 5$), 7.92 ± 0.03 ($n = 5$) on SERT, NET, DAT, respectively). Furthermore, the ability of **17** to block [^{3}H]5-HT, [^{3}H]NE, and [^{3}H]DA uptake was evaluated in functional uptake SPA assays using LLCPK cells stably transfected with human SERT, NET, or DAT. The compound inhibited monoamine uptake with $pIC_{50} = 8.4 \pm 0.28$ (SERT), 8.7 ± 0.30 (NET), 8.1 ± 0.05 (DAT) ($n = 3$), confirming that it binds to human SERT, NET, and DAT but also demonstrating that it can block the function of the transporters. The functional pIC_{50} observed in the DAT assay was in line with the affinity of the compound in the respective binding assay, while the functional pIC_{50} observed at NET was higher than the binding affinity for NET. In contrast, the functional potency at SERT was lower than its binding affinity for this transporter. In this latter case, a difference was expected, since the SERT uptake SPA assay is known to be particularly sensitive to test conditions (e.g., cell numbers) and, from previous experience,[3,4] most SERT blockers tested in uptake assays showed pIC_{50} lower than the corresponding affinity in the binding assay.

An additional critical step before performing in vivo experiments in preclinical models on this compound was the evaluation of its affinity in rat and mice SERT, NET, and DAT. The data obtained for the rat and the mouse (pK_i of 8.9, 8.6, and 8.0 for rat and pK_i of 8.8, 8.8, and 8.0 for mouse on SERT, NET, and DAT, respectively) are in good agreement with both the SPA and the filtration data generated on human recombinant cell lines.

Another important passage was to verify the selectivity of the compound on different targets. The compound demonstrated at least a 30-fold window with respect to its DAT affinity (i.e., its lower affinity among the three transporters) over more than 100 different receptors, enzymes, ion channels, and transporters when tested at Cerep.[8]

The pharmacokinetics and oral bioavailability of **17** were investigated in rat[9] showing good bioavailability ($F = 54\%$), moderate distribution volume ($V_d = 5.8$ L/kg), and moderate blood clearance (Clb = 48 (mL/min)/kg) resulting in a half-life of 1.7 h. The average brain/blood (B/B) concentration ratio was equivalent to 6.3 at 1 h.

Considering its overall balanced profile in terms of primary activity and PK properties, we decided to explore the in vivo behavior of the compound.

The first experiment was related to the increase in the extracellular concentration of monoamines, and this was measured in vivo;[9] microdialysis probes were implanted in the medial prefrontal cortex (mPFC) or nucleus accumbens (NA) in freely moving rats, and samples were analyzed with

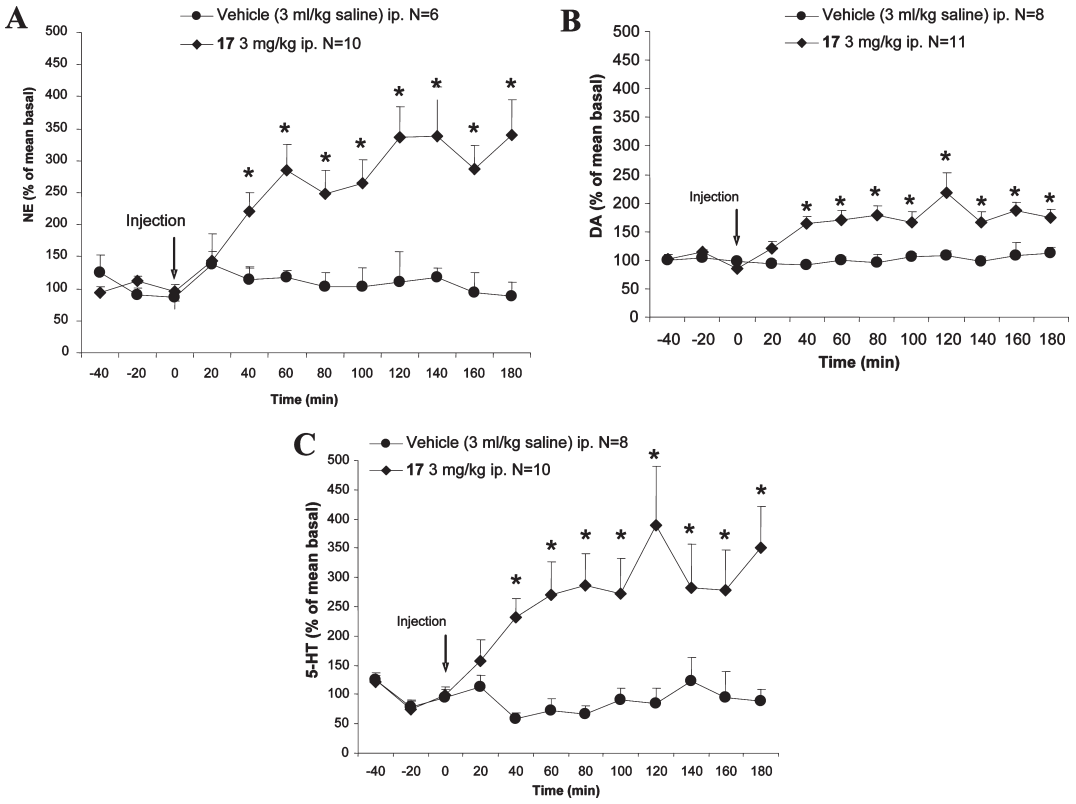

Figure 4. Time course of the effect of **17** (3 mg/kg, ip) on norepinephrine (A), dopamine (B), and serotonin (C) outflow in the rat nucleus accumbens. Arrow shows injection. Asterisk (∗) highlights significant difference vs respective vehicle time point (ANOVA with repeated measure of time followed, when appropriate, by planned comparison). Data are the mean ± SEM of neurotransmitter concentration expressed as percentage of basal values.

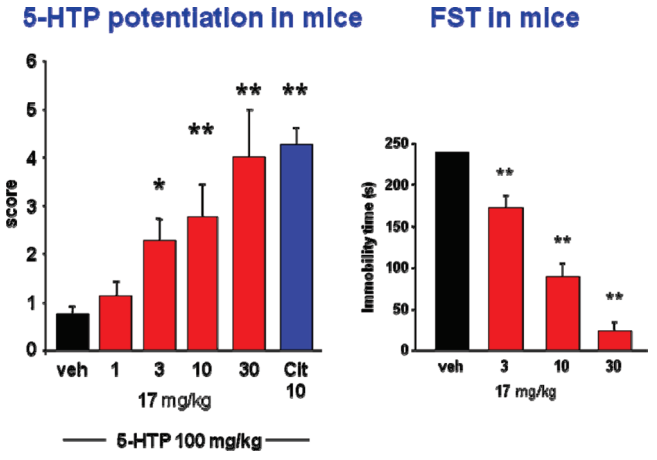

Figure 5. Effects of derivative **17** in the FST model (right) and in the 5-HTP model (left) in mice.

HPLC coupled to electrochemical detection for the measurement of NE, DA, and 5-HT concentrations. In the mPFC, **17** (3 mg/kg ip) induced a significant increase in NE, DA, and 5-HT levels that lasted throughout the experiment (Figure 3). In the NA, the same dose of the compound significantly augmented the outflow of NE, DA, and 5-HT (Figure 4). These results demonstrate that the acute administration of this molecule produced an increase in the extracellular levels of all monoamines in both the mPFC and NA in the rat.

Given these results, **17** was tested in two in vivo models in mice to acquire further information on its ability to block the monoamine transporters and therefore to produce an antidepressant-like effect.

Table 7. **17** ex Vivo SERT Occupancy in Rat Cortex (as %)

dose (mg/kg)	mean	SEM
vehicle	0	0.0
0.03	4.6	0.0
0.1	12.6	2.9
0.3	36.3	3.0
1	58.2	10.5
3	82.8	1.4
20	98.2	0.1

In the first of these experiments (Figure 5, left) it was tested in the 5-hydroxytryptophan (5-HTP) potentiation assay.[10] The compound was administered orally 2 h before the experiment. The results demonstrate that **17** significantly increased, in a dose dependent manner, 5-HTP stereotyped behavior at 3, 10, and 30 mg/kg. In the same study, the standard SSRI drug citalopram significantly increased 5-HTP stereotyped behavior. Accordingly, these data confirm in vivo the inhibition of the 5-HT transporter.

In the second experiment (Figure 5, right), **17** was evaluated for its potential antidepressant-like effect in the forced swimming test[11] (FST), which is sensitive to known antidepressant drugs. Once again, the compound was administered orally 2 h before the test in mice at 3, 10, and 30 mg/kg. As clearly seen in the figure, the compound significantly reduced immobility time at all doses as predicted by its in vitro affinity and PK profile.

Finally, two further experiments were performed to evaluate ex vivo occupancy of SERT elicited by **17**. In the first

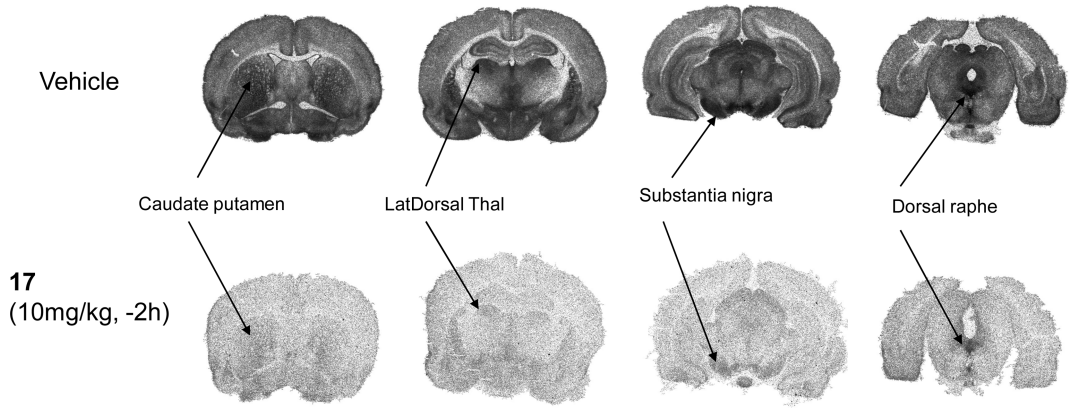

Figure 6. Autoradiographic study in rat brain: SERT occupancy after 10 mg/kg **17**.

study, the occupancy was determined 1 h after the administration of different doses of the compound from the binding of [^{3}H]citalopram to rat brain cortex. The results are reported in Table 7 and show a significant correlation between the doses of **17** and the percent of occupancy at SERT as expected by the PK and in vitro profile of the compound. In the second experiment, the evaluation of ex vivo SERT occupancy was performed using an autoradiographic technique, a method that allows quantification in many brain regions with high anatomical resolution. The compound was administered orally at 1, 3, and 10 mg/kg, and results for the top dose are reported in Figure 6. **17** showed high levels of SERT occupancy at the highest dose tested (10 mg/kg) in almost every brain region ($\gtrsim$95% occupancy in cortex, striatum, substantia nigra, and superior coulliculus and 87.92% occupancy in dorsal raphe), as expected by the SERT pK_i value and in agreement with previous data obtained with brain homogenates (Table 7).

Finally, the safety profile of the compound was studied in agreement with the requests of the regulatory authorities to proceed to dosing in human volunteers. The results will be provided in due course.

Conclusions

The discovery of the 6-aryl-1-[alkoxyalkyl]-3-azabicyclo-[4.1.0]heptane template as a potent and selective class of triple reuptake inhibitors is reported. The molecules belonging to this class are endowed with an excellent developability profile. They also perfectly fit the TRUI pharmacophore model recently described.

Derivative **17**, in particular, showed an excellent in vitro and in vivo profile, with clear activity in preclinical animal models correlated to the increase of the monoamines. MD and ex vivo experiments performed on this molecule clearly indicate its mode of action through monoamine uptake inhibition. Safety studies are in progress for a better characterization of this new scaffold.

Experimental Section

Biological Test Methods. In Vitro Studies. Filtration Binding Assay for Human Recombinant SERT, NET, and DAT. Filtration binding assays were run using membranes prepared from LLCPK cells stably transfected with each of the three human transporters. Filtration [^{3}H]citalopram binding assay for human SERT (hSERT) was conducted in a deep-well 96-well plate in a total volume of 404 μL/well by adding 4 μL of test compound (100$\times$ solution in neat DMSO) or DMSO (to define total binding) or a final concentration of 10 μM fluoxetine (to define nonspecific binding, NSB), 200 μL of 0.25 nM [*N*-methyl-^{3}H]-citalopram (Amersham Biosciences, 80 Ci/mmol), and 200 μL of hSERT-LLCPK membranes (about 2.5 μg protein/well). After 2 h at room temperature the reaction was stopped by rapid filtration through GF/B UniFilter 96 filter plate (Perkin-Elmer) presoaked in 0.5% polyethyleneimine (PEI) using a Perkin-Elmer FilterMat-196 harvester. The filter plate was washed 3 times with 1 mL/well ice-cold 0.9% NaCl solution, dried, and finally an amount of 50 μL of Microscint 20 (Perkin-Elmer) were added to each well. The radioactivity was counted using TopCount liquid scintillation counter (Packard-Perkin-Elmer) and recorded as counts per minute (CPM). Data analysis was performed by using a four-parameter logistic equation with GraphPad PRISM software, and pK_i was calculated from pIC_{50} by using the Cheng–Prusoff equation. Competition binding assay for human NET (hNET) was conducted essentially as previously reported for SERT except for the use of hNET-LLCPK cell membranes (4.8 μg/well), 1.5 nM [*N*-methyl-^{3}H]nisoxetine as radioligand (Amersham Biosciences, 84 Ci/mmol), and 10 μM desipramine for NSB. Finally, the same procedure was also adopted for human DAT (hDAT) competition binding assay but using hDAT/LLCPK cell membranes (9.6 μg/well), 10 nM [*N*-methyl-^{3}H]WIN-35,428 (Perkin-Elmer, 85.6 Ci/mmol), and 10 μM GBR-12909 for NSB.

Filtration Binding for Rat Native SERT, NET, and DAT and Mouse Native SERT. Filtration binding studies were carried out on rat and mouse brain native tissue. The affinity of the compound was determined on rat or mouse cortex for SERT, on rat hippocampus for NET, and on rat striatum for DAT, using the appropriate radioligand. Competition binding assays for rat and mouse SERT, rat NET, and rat DAT were conducted essentially as previously reported for human recombinant monoamine transporters but using a different amount of membranes (20 and 7 μg of protein/well for rat and mouse SERT binding, 40 and 20 μg/well for rat NET and DAT binding, respectively).

hERG–[^{3}H]Dofetilide Binding Assay. hERG activity was measured using [^{3}H]dofetilide binding in a scintillation proximity assay (SPA) format. The activity was measured with a PerkinElmer Viewlux imager.

SPA Binding for Human Recombinant SERT, NET, and DAT. The affinity of the compounds to the human transporters has been assessed with radioligand displacement binding of [^{3}H]citalopram, [^{3}H]nisoxetine, and [^{3}H]WIN-35,428 for SERT, NET, and DAT in BacMam-recombinant human SERT, NET, and DAT membranes with the SPA technology. Briefly, 0.3 μL of test compound was added to 30 μL of the SPA mixture containing 1 mg/mL SPA (GE HealthCare, RPNQ0260) beads (SERT) or 2 mg/mL SPA beads (NET and DAT), 6 or 40 or 20 μg/mL SERT or NET or DAT BacMam membranes, 0.02% Pluronic F-127, 3 nM [^{3}H]citalopram or 10 nM [^{3}H]nisoxetine or 10 nM [^{3}H]WIN-35,428 for SERT or NET or DAT binding SPA in the

assay buffer (20 mM HEPES, 145 mM NaCl, 5 mM KCl, pH 7.4). Incubation was performed overnight at room temperature. Bound radioactivity was measured with the Viewlux instrument. Data analysis was performed by using a four-parameter logistic equation with ActivityBase software, and pK_i was calculated from pIC_{50} by using the Cheng−Prusoff equation.

Functional Uptake for SERT, NET, and DAT. The potency of the compounds in blocking the [^{3}H]serotonin, [^{3}H]noradrenalin, and [^{3}H]dopamine uptake was evaluated in a functional uptake SPA assay on LLCPK cells stably transfected with human SERT, NET, and DAT. Briefly, 0.2 μL of test compound was added to 10 μL of the bead−cell SPA mixture containing 1.5 mg/mL SPA beads (SERT and NET) or 2 mg/mL of SPA beads (DAT), 25 000 or 50 000 or 75 000 cell/well of SERT or NET or DAT LLCPK cells, 0.02% Pluronic F-127 in the assay buffer (20 mM HEPES, 145 mM NaCl, 5 mM KCl, pH 7.4). The uptake was started by the substrate addition of 10 μL of 35 nM [^{3}H]serotonin or 45 nM [^{3}H]noradrenalin or 75 nM [^{3}H]dopamine for SERT or NET or DAT uptake SPA. Incubation was performed at room temperature for 1 h. Uptake was measured with the Viewlux instrument, and data analysis was performed as before.

P450 CYPEX Assay. Inhibition (IC_{50}) of human CYP1A2, 2C9, 2C19, 2D6, and 3A4 was determined using Cypex Bactosomes expressing the major human P450s. A range of concentrations (0.1, 0.2, 0.4, 1, 2, 4, and 10 μM) of test compound were prepared in methanol and preincubated at 37 °C for 10 min in 50 mM potassium phosphate buffer (pH 7.4) containing recombinant human CYP450 microsomal protein (0.1 mg/mL; Cypex Limited, Dundee, U.K.) and probe-fluorescent substrate. The final concentration of solvent was between 3% and 4.5% of the final volume. Following preincubation, NADPH regenerating system (7.8 mg of glucose 6-phosphate, 1.7 mg of NADP, and 6 units of glucose 6-phosphate dehydrogenase/mL of 2% (w/v) $NaHCO_3$; 25 μL) was added to each well to start the reaction. Production of fluorescent metabolite was then measured over a 10 min time course using a Spectrafluor Plus plate reader. The rate of metabolite production (AFU/min) was determined at each concentration of compound and converted to a percentage of the mean control rate using Magellan (Tecan software). The inhibition (IC_{50}) of each compound was determined from the slope of the plot using Grafit, version 5 (Erithacus software, U.K.). Miconazole was added as a positive control to each plate. CYP450 isoform substrates used were ethoxyresorufin (ER, 1A2, 0.5 μM), 7-methoxy-4-triflouromethylcoumarin-3-acetic acid (FCA, 2C9, 50 μM), 3-butyryl-7-methoxycoumarin (BMC, 2C19, 10 μM), 4-methylaminomethyl-7-methoxycoumarin (MMC, 2D6, 10 μM), diethoxyflourescein (DEF, 3A4, 1 μM), and 7-benzyloxyquinoline (7-BQ, 3A4, 25 μM). The test was performed in three replicates.

Intrinsic Clearance (Cli) Assay. Intrinsic clearance (Cli) values were determined in rat and human liver microsomes. Test compounds (0.5 μM) were incubated at 37 °C for 30 min in 50 mM potassium phosphate buffer (pH 7.4) containing 0.5 mg of microsomal protein/mL. The reaction was started by addition of cofactor (NADPH, 8 mg/mL). The final concentration of solvent was 1% of the final volume. At 0, 3, 6, 9, 15, and 30 min an aliquot (50 μL) was taken, quenched with acetonitrile containing an appropriate internal standard, and analyzed by HPLC−MS/MS. The intrinsic clearance (Cli) was determined from the first-order elimination constant by nonlinear regression using Grafit, version 5 (Erithacus software, U.K.), corrected for the volume of the incubation and assuming 52.5 mg of microsomal protein/g of protein for all species. Values for Cli were expressed as (mL/min)/g of protein. The lower limit of quantification of clearance was determined to be when $<15\%$ of the compound had been metabolized by 30 min, and this corresponded to a Cli value of 0.5 (mL/min)/g of protein. The upper limit was 50 (mL/min)/g of protein.

5-HTP Potentiation Test. The administration of the precursor of 5-hydroxytryptophan (5-HTP) to mice leads to a serotonergic syndrome characterized by stereotypic behavior. The combination monoamine reuptake inhibitors with subthreshold doses of 5-HTP has been proposed as a model to evaluate in vivo effects of drug acting at the serotonin transporter (Ortmann, 1980).

Mice were pretreated with **17** 120 min before an intraperitoneal (ip) injection of 5-HTP (100 mg/kg) and placed individually into a perspex box (20.5 cm × 20.5 cm × 34 cm). Experiments were videotaped, and the following behaviors over 30 min were scored: aimless hyperlocomotor activity (aHLMA), abduction of hind limbs (HLA), flat body posture (FBP), head twiches/tremor (HT), body tremor (BT). Each behavior was scored either present (scored = 1) or absent (scored = 0) by an observer blind to the drug treatment.

Forced Swimming Test. The mouse forced swimming test (Porsolt et al., 1977) is widely used as an animal model for detecting and screening antidepressant activity. Mice were dropped individually into glass cylinders (height 25 cm, diameter 10 cm) containing 10 cm of water maintained at 25 ± 1 °C and left there for 6 min. A mouse was judged immobile when it floated in an upright position and made only small movements to keep its head above water. The duration of immobility was recorded during the last 4 min of the 6 min testing period. All experiments were videotaped, and the observer was unaware of the drug treatment scores immobility.

Compound **17** was administered orally 120 min before test.

MD and Locomotor Activity Data. Animals. Male CD rats (Charles River, Italy) weighing between 280 and 310 g at the beginning of the experiment were housed in constant conditions of temperature (21 ± 1 °C) and moisture under a 12 h light/dark cycle with water and food available ad libitum. They were handled everyday to get accustomed to manipulation and presence of researchers.

Intracerebral Microdialysis Surgery. Animals were anesthetized with proper concentrations of medetomidine hydrochloride (Domitor) and xylazine (Zoletil), while carpofren (Rymadil) was injected to induce analgesia. They were then placed on a stereotaxic apparatus for small animals. A guide cannula was lowered and positioned above the left medial prefrontal cortex (anteroposterior 3.2 mm, lateral 0.5 mm, dorsoventral 1.8 mm from bregma) or nucleus accumbens (anterior, +1.7 mm; ventral, −6.0 mm; mediolateral, 1.2 mm from bregma) and secured to the skull using dental cement, anchored by four stainless steel screws. A removable stainless steel stylet was placed inside the cannula to maintain its patency throughout the experimental period. Following surgery the animals were injected with atipamezole hydrochloride (Antisedan) and Rubrocillin antibiotic and housed in single cages for 1 week to recover.

Microdialysis Experiment. The day before the experiment the stylette was removed from the guide cannula, and a microdialysis probe with a 2 or 4 mm long membrane (depending on the region) was inserted (MAB 4 Agntho's, Sweden). The following day microdialysis experiments were performed in their home cage. Both inlet and outlet of the probe were attached with FEP tubings (dead volume of 1.2 μL/10 cm) to a dual quartz lined two-channel liquid swivel (model 375/D/22QM Instech Labs, Plymouth Meeting, PA) mounted on a low mass spring counterbalanced arm (MCLA, Instech). One channel was connected to a gas tight syringe (Hamilton 1002 LTN 2.5 mL, Bonaduz, Switzerland) on a microinfusion pump (The Univentor 802 syringe pump) to deliver artificial cerebrospinal fluid (KCl 2.5 mM, NaCl 125 mM, $CaCl_2$ 1.3 mM, $MgCl_2$ 1.18 mM, Na_2HPO_4 2 mM, pH 7.4, with H_3PO_4 85%) at a steady flow rate of 1.1 μL/min, and the second channel was connected to a refrigerated fraction collector (Univentor 820 microsampler) containing microtubes with 3 μL of 1 mM oxalic acid solution. Length of the outlet tubing was calculated to achieve a 20 min delay of sample collection. Samples were collected every 20 min and frozen in dry ice for subsequent HPLC analysis. Two hours of perfusion were allowed before starting the experiment.

Probe Localization. The position of the probe in the brain areas was verified at the end of each experiment. A blue dye was injected through a probe without the dialysis membrane, and the brains were then removed and coronally sectioned at the level of the PFC or NAc. Trace localization was visually identified through comparison with a stereotaxic atlas of rat brain (Paxinos and Watson, 2005). Animals with incorrect probe position were discarded from the final analysis.

HPLC Procedure. NA, DA, and 5-HT concentrations were determined in dialysate samples by HPLC with electrochemical detection (Antec Decade). Separation was achieved using a mobile phase consisting of 12 mM Na_2HPO_4, 88 mM NaH_2PO_4, 5 mM NaCl, 0.1 mM EDTA·Na_2, 20% MeOH, 10% MeCN, pH 6.00 ± 0.05. Chromatographic data were acquired and processed through Empower software.

Data Analysis. For each animal absolute neurochemical data in picogram were transformed to percent values vs average of the three basal values. They were preliminarily analyzed with a 2D Box & Whiskers plot to determine and eliminate outlier and extreme values. Data eliminated were substituted with the mean of the same group at the same time. Final data were analyzed with two-way ANOVA for repeated measures with treatment and time as factors. Whenever allowed, preplanned post hoc multiple comparisons were applied to compare time points of different treatments.

Concurrent general motor activity was measured through an automated digital video analysis of animal movements (ViewPoint). Data were analyzed as previously described for microdialysis data.

Ex Vivo Autoradiography of SERT after Oral Administration of 17 in Rat. Sprague−Dawley rats were acutely treated with **17** at 1, 3, and 10 mg/kg po (−90 min), and spontaneous locomotor activity was recorded for 30 min. At the end of the test, animals were sacrificed and brains were quickly removed and frozen and processed for in vitro autoradiography of SERT (2nM [^{3}H]citalopram).

General Chemical Procedures. Proton magnetic resonance (NMR) spectra are typically recorded either on a Varian instrument at 300, 400, or 500 MHz or on a Bruker instrument at 300 and 400 MHz. Chemical shifts are reported in ppm (δ) using the residual solvent line as internal standard. Splitting patterns are designated as follows: s, singlet; d, doublet; t, triplet; q, quartet; m, multiplet; b, broad. The NMR spectra were recorded at a temperature ranging from 25 to 90 °C. When more than one conformer was detected, the chemical shifts for the most abundant one was reported. Mass spectra (MS) are typically taken on a 4 II triple quadrupole mass spectrometer (Micromass UK) or on a Agilent MSD 1100 mass spectrometer, operating in ES (+) and ES (−) ionization mode or on an Agilent LC/MSD 1100 mass spectrometer, operating in ES (+) and ES (−) ionization mode coupled with an HPLC Agilent 1100 series instrument. In the mass spectra only one peak in the molecular ion cluster is reported. When HPLC walk-up retention time is reported, the analysis is done on a HPLC Agilent 1100 series instrument with the following conditions: column, Luna C18 100A 50 mm × 2 mm, 3 μm; mobile phase, (MeCN + 0.05% TFA)/(H_2O + 0.05% TFA), gradient from 0/100 to 95/5 in 8 min; flux 1 mL/min. Flash silica gel chromatography was carried out on silica gel 230−400 mesh (supplied by Merck AG Darmstadt, Germany) or over Varian Mega Be−Si prepacked cartridges or over prepacked Biotage silica cartridges.

SPE-SCX cartridges are ion exchange solid phase extraction columns supplied by Varian. The eluent used with SPE-SCX cartridges is methanol followed by 2 N ammonia solution in methanol. In a number of preparations, purification was performed using either Biotage manual flash chromatography (Flash+) or automatic flash chromatography (Horizon, SP1) systems. All these instruments work with Biotage silica cartridges. SPE-Si cartridges are silica solid phase extraction columns supplied by Varian.

The enantiomeric purity of each single enantiomer obtained after preparative chromatography on chiral columns was always verified on analytical column.

The purity of the compounds reported in the manuscript was established through HPLC methodology. All the compounds reported in the manuscript have a purity of >95%.

General Synthetic Procedures. 1-(1,1-Dimethylethyl) 3-Methyl-4-hydroxy-5,6-dihydro-1,3(2*H*)-pyridinedicarboxylate (54). To a stirred solution of methyl 4-oxo-3-piperidinecarboxylate hydrochloride in dry DCM at 0 °C and under a nitrogen atmosphere, TEA was added dropwise over 5 min. The mixture was stirred at 0 °C for 5 min, then allowed to reach room temperature. Bis(1,1-dimethylethyl) dicarbonate was then added, and the solution was left stirring overnight at room temperature under nitrogen. After quenching and workup, the crude product was purified by flash chromatography (eluting with ethyl acetate/cyclohexane 1:3) to give the title compound. NMR (^{1}H, $CDCl_3$): δ 11.95−12.02 (m, 1 H), 4.07 (br s, 2 H), 3.77−3.82 (m, 3 H), 3.58 (t, 2 H), 2.34−2.43 (m, 2 H), 1.46−1.50 (m, 9 H).

1-(1,1-Dimethylethyl) 3-Methyl-4-{[(trifluoromethyl)sulfonyl]-oxy}-5,6-dihydro-1,3(2*H*)-pyridinedicarboxylate (55). To a stirred solution of 1-(1,1-dimethylethyl) 3-methyl-4-oxo-1,3-piperidinedicarboxylate (**54**) in dry DMF at 0 °C and under a nitrogen atmosphere, NaH (60% on mineral oil) was added portionwise. The reaction mixture was stirred at 0 °C for 10 min. Then a solution of *N*-phenyl-bis(trifluoromethanesulfonimide) in dry DMF was added dropwise, and stirring was continued for 0.5 h. After quenching and workup, the solvent was removed under reduced pressure and the compound was purified by flash chromatography to give the title compound. NMR (^{1}H, $CDCl_3$): δ 4.29 (br s, 2 H), 3.82−3.87 (m, 3 H), 3.64 (t, 2 H), 2.50−2.57 (m, 2 H), 1.46−1.52 (m, 9 H). MS (*m*/*z*): 390 $[MH]^+$, 412 $[MNa]^+$.

1-(1,1-Dimethylethyl) 3-Methyl-4-(3,4-dichlorophenyl)-5,6-dihydro-1,3(2*H*)-pyridinedicarboxylate (56). To a mixture of 1-(1,1-dimethylethyl) 3-methyl-4-{[(trifluoromethyl)sulfonyl]-oxy}-5,6-dihydro-1,3(2*H*)-pyridinedicarboxylate (**55**), 3,4-dichlorophenylboronic acid, and $Pd(PPh_3)_4$ under nitrogen were added toluene, ethanol, and Na_2CO_3 (aqueous 2 M solution) in sequence. The mixture was stirred at 80 °C for 1 h, and then the reaction mixture was allowed to reach room temperature. After quenching and workup, the crude product was purified by flash chromatography (eluting with ethyl acetate/cycloexane 1:3) to give the title compound. NMR (^{1}H, $CDCl_3$): δ 7.42 (d, 1 H), 7.25 (d, 1 H), 6.98 (dd, 1 H), 4.26 (br s, 2 H), 3.61 (t, 2 H), 3.55−3.58 (m, 3 H), 2.47 (br s, 2 H), 1.50−1.54 (m, 9 H).

1,1-Dimethylethyl 4-(3,4-Dichlorophenyl)-5-(hydroxymethyl)-3,6-dihydro-1(2*H*)-pyridinecarboxylate (57). To a stirred solution of 1-(1,1-dimethylethyl) 3-methyl-4-(3,4-dichlorophenyl)-5,6-dihydro-1,3(2*H*)-pyridinedicarboxylate (**56**) in dry diethyl ether under nitrogen atmosphere at −20 °C, $LiAlH_4$ (1 M in diethyl ether) was added dropwise over 1 min. The reaction mixture was left stirring at −20 °C for 15 min, then quenched with aqueous saturated NH_4Cl solution and diethyl ether After workup, the crude product was purified by flash chromatography (eluting with ethyl acetate/cycloexane 1:3) to give the title compound. NMR (^{1}H, DMSO-d_6): δ 7.62 (d, 1 H), 7.56 (d, 1 H), 7.26 (dd, 1 H), 4.90 (t, 1 H), 4.02 (br s, 2 H), 3.79 (d, 2 H), 3.49 (t, 2 H), 2.35 (br s, 2 H), 1.42−1.46 (m, 9 H).

6-(3,4-Dichlorophenyl) 1-[(Methyloxy)methyl]-3-azabicyclo-[4.1.0]heptane-3-carboxylate (17). To a stirred solution of CH_2I_2 in dry CH_2Cl_2 under argon atmosphere at 0 °C $ZnEt_2$ (1 M in hexane) was added dropwise. The mixture was stirred at 0 °C for 20 min and then cooled at −20 °C. A solution of **57** in dry CH_2Cl_2 was added dropwise, and the reaction mixture was stirred for an additional 30 min, then 40 min at 0 °C, and overnight at room temperature. After quenching and workup, the crude product was quickly purified by flash chromatography (eluting with ethyl acetate/cycloexane 1:3). This intermediate was dissolved in dry CH_2Cl_2 under argon atmosphere and stirred at room temperature. Bis(1,1-dimethylethyl) dicarbonate was

added, and the mixture was left stirring overnight. After quenching and workup the material was purified by flash chromatography (eluting with diethyl ether/*n*-hexane 1:2 to 1:1) to give the 1,1-dimethylethyl 4-(3,4-dichlorophenyl)-5-(hydroxymethyl)-3,6-dihydro-1(2*H*)-pyridinecarboxylate intermediate. This material was dissolved in dry THF under argon atmosphere at 0 °C. NaH (60% on mineral oil) was added in one portion, and the stirring continued for 30 min. After this period CH_3I was added dropwise and the mixture was allowed to reach room temperature and stirred for 1.5 h. After quenching and workup, the material was purified by flash chromatography (eluting with diethyl ether/*n*-hexane 40:60) to give the 1,1-dimethylethyl 4-(3,4-dichlorophenyl)-5-[(methyloxy)methyl]-3,6-dihydro-1(2*H*)-pyridinecarboxylate intermediate. Finally, deprotection with TFA in CH_2Cl_2 was performed at 0 °C to give the title compound. NMR (^{1}H, DMSO-d_6): δ 8.71 (br s, 2 H), 7.73 (d, 1 H), 7.59 (d, 1 H), 7.41 (dd, 1 H), 3.45 (d, 1 H), 3.09−3.16 (m, 2 H), 3.04 (s, 3 H), 2.92 (d, 1 H), 2.73−2.82 (m, 1 H), 2.66 (d, 1 H), 2.01−2.17 (m, 2 H), 1.22−1.29 (m, 2 H); MS (*m*/*z*): 286 $[MH]^+$

1,1-Dimethylethyl 4-{[(Trifluoromethyl)sulfonyl]oxy}-3,6-dihydro-1(2*H*)-pyridinecarboxylate (61). To a stirred solution of diisopropylamine in dry THF at −78 °C and under a nitrogen atmosphere, butyllithium (2.5 M in hexane) was added. The reaction mixture was stirred at −78 °C for 15 min. DMPU (1.8 mL) and a solution of 1,1-dimethylethyl 4-oxo-1-piperidinecarboxylate (**60**) in THF were added, and the reaction mixture was stirred at −78 °C for 2 h. Then a solution of *N*-phenylbis(trifluoromethanesulfonimide) in THF was added and stirring was continued at 0 °C for 9 h and at room temperature per 16 h. The solvent was removed under reduced pressure and the crude purified by flash chromatography (eluting with ethyl acetate/cycloexane 2:8) to give the title compound. NMR (^{1}H, $CDCl_3$): δ 5.79 (br s, 2 H), 4.07 (m, 2 H), 3.65 (m, 2 H), 2.47 (m, 2 H), 1.50 (s, 9 H).

3-(1,1-Dimethylethyl) 7-Ethyl 6-(3,4-dichlorophenyl)-3-azabicyclo[4.1.0]heptane-3,7-dicarboxylate (63). To a mixture of **61**, 3,4-dichlorophenylboronic acid, and $Pd(PPh_3)_4$ under nitrogen were added toluene, ethanol, and Na_2CO_3 in sequence. The mixture was stirred at 80 °C for 2 h. Then it was allowed to reach room temperature. After quenching and workup, the intermediate was purified by flash chromatography (eluting with ethyl acetate/cycloexane 1:9) to give intermediate **62**. The compund was dissolved in CH_2Cl_2, and rhodium acetate was added. The mixture was heated at 40 °C. A solution of ethyl diazoacetate in CH_2Cl_2 was added with a syringe pump in 4 h, maintaining the internal temperature at 50 °C during the addition. The solvent was removed under reduced pressure and the crude purified by flash chromatography (eluting with ethyl acetate/cycloexane 2:8) to give the intermediate title compound (MS (*m*/*z*): 414 $[MH]^+$).

6-(3,4-Dichlorophenyl)-7-[(methyloxy)methyl]-3-azabicyclo-[4.1.0]heptane (20). To a stirred solution of **63** in dry toluene under a nitrogen atmosphere at −20 °C, $LiAlH_4$ (1 M in diethyl ether) was added dropwise. The reaction mixture was left stirring at −20 °C for 1 h. After quenching and workup, the crude intermediate **64** was obtained (MS (*m*/*z*): 372 $[MH]^+$). To a stirred solution of this product in dry DMF under nitrogen atmosphere at 0 °C, NaH (60% on mineral oil) was added. The mixture stirred for 30 min at 0 °C. Methyl iodide was added. The mixture was allowed to reach room temperature, and it was stirred for an additional 2 h. After quenching and workup, the crude was treated with TFA in CH_2Cl_2 at 0 °C to give the title compound after careful column chromatography. NMR (^{1}H, $CDCl_3$): δ 7.37 (d, 1 H), 7.33 (d, 1 H), 7.13 (dd, 1 H), 4.01 (dd, 1 H), 3.78 (dd, 1 H), 3.44 (s, 3H), 3.32 (m, 1H), 3.17 (m, 1H), 2, 84 (m, 1H), 2.59 (m, 1H), 2.04 (m, 1H), 1.88 (m, 1H), 1.37 (m, 2H).

6-(4-Chlorophenyl)-1-[(methyloxy)methyl]-3-azabicyclo[4.1.0]-heptane (21). NMR (^{1}H, $CDCl_3$): δ ppm 7.25 (s, 4 H), 3.30 (d, 1 H), 3.08−3.14 (m, 4 H), 2.85−2.91 (m, 2 H), 2.63−2.80 (m, 2 H), 1.81−1.99 (m, 2 H), 0.99−1.05 (m, 2 H).

1-[(Methyloxy)methyl]-6-{4-[(trifluoromethyl)oxy]phenyl}-3-azabicyclo[4.1.0]heptane Hydrochloride (22). NMR (^{1}H, MeOH-d_4): δ ppm 7.52 (d, 2 H), 7.24 (d, 2 H), 3.72 (d, 1 H), 3.27 (d, 1 H), 3.25 −3.21 (m, 1 H), 3.16 −3.12 (m, 3 H), 3.07 (d, 1 H), 2.97−2.84 (m, 1 H), 2.74 (d, 1 H), 2.32−2.12 (m, 2 H), 1.31 (d, 1 H), 1.22 (d, 1 H).

6-(3-Chloro-4-fluorophenyl)-1-[(methyloxy)methyl]-3-azabicyclo[4.1.0]heptane Hydrochloride (23). NMR (^{1}H, DMSO-d_6): δ ppm 8.28 (s, 1 H), 7.66 (d, 1 H), 7.25−7.47 (m, 2 H), 3.41 (d, 1 H), 3.01−3.14 (m, 5 H), 2.92 (d, 1 H), 2.75 (d, 1 H), 2.68 (d, 1 H), 1.98−2.10 (m, 2 H), 1.17−1.26 (m, 2 H). MS (*m*/*z*): 270 $[MH]^+$.

6-[4-Chloro-3-(trifluoromethyl)phenyl]-1-[(methyloxy)methyl]-3-azabicyclo[4.1.0]heptane (24). NMR (^{1}H, $CDCl_3$): δ 7.72 (d, 1 H), 7.48−7.53 (m, 1 H), 7.42−7.46 (m, 1 H), 3.42 (d, 1 H), 3.08−3.14 (m, 4 H), 3.04 (d, 1 H), 2.81−2.90 (m, 1 H), 2.66−2.76 (m, 2 H), 1.97−2.06 (m, 1 H), 1.85−1.93 (m, 2 H), 1.11 (d,1 H), 1.04 (d, 1 H). MS (*m*/*z*): 320 $[MH]^+$.

6-[3-Chloro-4-(trifluoromethyl)phenyl]-1-[(methyloxy)methyl]-3-azabicyclo[4.1.0]heptane (25). NMR (^{1}H, $CDCl_3$): δ ppm 7.71 (s, 1 H), 7.46 (dd, 2 H), 3.40 (d, 1 H), 3.12 (s, 3 H), 2.99−3.10 (m, 2 H), 2.76−2.91 (m, 1 H), 2.65−2.76 (m, 2 H), 1.91−2.07 (m, 2 H), 1.79−1.91 (m, 1 H), 1.10 (d, 1 H), 1.02 (d, 1 H). MS(*m*/*z*): 320 $[MH]^+$.

1-[(Methyloxy)methyl]-6-(2-naphthalenyl)-3-azabicyclo[4.1.0]-heptane (26). NMR (^{1}H, $CDCl_3$): δ 7.77−7.86 (m, 3 H), 7.72−7.76 (m, 1 H), 7.42−7.52 (m, 3 H), 3.37 (d, 1 H), 3.18 (d, 1 H), 3.10 (s, 3 H), 3.02 (d, 1 H), 2.80−2.89 (m, 2 H), 2.70−2.79 (m, 1 H), 1.96−2.08 (m, 2 H), 1.25 (d, 1 H), 1.11 (d, 1H). MS(*m*/*z*): 268 $[MH]^+$.

6-(3,4-Dichlorophenyl)-1-[(ethyloxy)methyl]-3-azabicyclo[4.1.0]-heptane Hydrochloride (29). NMR (^{1}H, MeOH-d_4): δ 7.58 (d, 1 H), 7.38 (d, 1 H), 7.25 (dd, 1 H), 3.64 (d, 1 H), 3.15 (m, 5 H), 2.79 (m, 1 H), 2.57 (d, 1 H), 2.11 (m, 2 H), 1.19 (d, 1 H), 1.12 (d, 1 H), 0.98 (t, 3 H). MS (*m*/*z*): 300 $[MH]^+$.

6-(3,4-Dichlorophenyl)-1-{[(2,2,2-trifluoroethyl)oxy]methyl}-3-azabicyclo[4.1.0]heptane (32). NMR (^{1}H, $CDCl_3$): δ 7.5 (s, 1 H) 7.45 (d, 1 H) 7.35 (m, 1 H), 3.9 (d, 2 H) 3.7 (d, 1 H) 3.6 (m, 2 H) 3.25 (d, 1 H) 3.15 (m, 2 H) 2.3 (m, 1 H) 2.2 (m, 1 H) 1.25 (m, 2 H).

6-(3,4-Dichlorophenyl)-4-methyl-1-[(methyloxy)methyl]-3-azabicyclo[4.1.0]heptane (40). NMR (^{1}H, $CDCl_3$): δ 7.46 (d, 1 H), 7.33 (d, 1 H), 7.20 (dd, 1 H), 3.54 (d, 1 H), 3.06−3.17 (m, 3 H), 2.89−3.01 (m, 2 H), 2.72 (d, 1 H), 2.27−2.53 (m, 1 H), 1.91−2.07 (m, 1 H), 1.27−1.46 (m, 1 H), 1.04 (d, 3 H), 0.87−0.98 (m, 2 H). MS (*m*/*z*): 300 $[M + H]^+$.

6-(3,4-Dichlorophenyl)-1-[1-(methyloxy)-3-buten-1-yl]-3-azabicyclo[4.1.0]heptane (45). The previously described 1,1-dimethylethyl 6-(3,4-dichlorophenyl)-1-(hydroxymethyl)-3-azabicyclo-[4.1.0]heptane-3-carboxylate was dissolved in dry CH_2Cl_2 and stirred under a nitrogen atmosphere at 0 °C. After 10 min, Dess−Martin periodinane was added portionwise and the mixture slowly warmed to room temperature and stirred for 1 h. After quenching and workup, the intermediate formyl derivative (1,1-dimethylethyl) 6-(3,4-dichlorophenyl)-1-formyl-3-azabicyclo-[4.1.0]heptane-3-carboxylate) was obtained as a yellow oil (314 $[MH - 56]^+$). The compound was dissolved in THF at 20 °C, and to the solution bromo(2-propen-1-yl)magnesium was added. After quenching and workup, the residue was purified by chromatography (c-Hex/EtOAc 0−30%, 100 g silica column) to give two diastereomers as oils. One diastereoisomer was dissolved in dry DMF, and NaH was added at 0 °C, followed by the addition of methyl iodide. After quenching and workup, the residue was purified by chromatography (CyH/EtOAc from 0% EtOAc to 30%), and it was dissolved in CH_2Cl_2. TFA was added, and the mixture was stirred at 0 °C for 30 min. After quenching and workup the compound was purified by SCX to give the title compound. NMR(^{1}H, CDCl3): δ 7.53 (s, 1H), 7.38 (d, 1H), 7.27 (m, 1H), 5.73 (m, 1H), 5.04 (d, 1H), 4.99 (d, 1H), 3.50 (d, 1H), 2.99 (s, 3H), 2.97 (d, 1H), 2.85 (m. 1H), 2.59 (m, 1H), 2.40 (m, 1H), 2.25 (m, 1H), 2.17 (m, 1H), 1.94 (t, 2H), 1.00 (m, 2H). MS (*m*/*z*) = 326 $[MH]^+$.

6-(3,4-Dichlorophenyl)-3-methyl-1-[(methyloxy)methyl]-3-azabicyclo[4.1.0]heptane (47). NMR (^{1}H, $CDCl_3$): δ 7.44 (d, 1 H), 7.35 (d, 1 H), 7.18 (dd, 1 H), 3.15 (s, 3 H), 2.90 (dd, 2 H), 2.78 (d, 1 H), 2.70 (d, 1 H), 2.23−2.30 (m, 5 H), 1.96−2.13 (m, 2 H), 1.05 (d, 1 H), 1.01 (d, 1 H). MS (m/z): 300 $[M + H]^+$.

3-(3,4-Dichlorophenyl)-6-azatricyclo[4.2.1.0^{1,3}]nonane (49, 50). The previously described 1,1-dimethylethyl 6-(3,4-dichlorophenyl)-1-(hydroxymethyl)-3-azabicyclo[4.1.0]heptane-3-carboxylate was transformed into the corresponding ethyl ester according to WO2008/031772. The solution was treated with triethylsilane, followed by TFA. The reaction mixture was stirred for 2 h at room temperature. After quenching and workup, the obtained compound was dissolved in dry CH_2Cl_2. The solution was treated with Boc_2O and TEA. After quenching and workup, the intermediate compound was hydrolyzed with potassium *tert*-butoxide to give the corresponding carboxylic acid. This compound was dissolved in dry CH_2Cl_2. TEA, oxalyl chloride, and DMF were added at 0 °C under a nitrogen atmosphere. The mixture was stirred at 0 °C for 30 min and then at room temperature for 1 h. The reaction mixture was evaporated under reduced pressure. The residue was dissolved in a mixture of anhydrous THF and anhydrous acetonitrile, and to this mixture was added TMS-diazomethane (2 M in diethyl ether) at 0 °C under a nitrogen atmosphere. The mixture was stirred at 0 °C for 1 h and then for an additional 2 h at room temperature. After quenching and workup, this compound was dissolved in THF/water (3:1). Silver benzoate was added and the obtained mixture sonicated using an ultrasound bath. After quenching and workup, the compound was taken up in methanol and CH_2Cl_2. Then TMS-diazomethane (2 M in hexane) was added dropwise under an atmosphere of nitrogen at room temperature and the mixture was stirred for 2 h. The resulting methyl ester was dissolved in dry toluene and the obtained solution cooled to −20 °C. Then $LiAlH_4$ (2 M solution in THF) was added dropwise and the reaction mixture was stirred at −20 °C for 1 h to give the primary alcohol. The compound was dissolved in dry CH_2Cl_2. Mesyl-Cl and DIPEA were added at 0 °C. The reaction mixture was stirred at room temperature for 1 h. After quenching and workup, the new compound was dissolved in dry CH_2Cl_2. TFA was added at 0 °C and the reaction mixture stirred at room temperature for 5 h. Finally, after quenching and workup, the obtained derivative was dissolved in dry DMF, sodium iodide was added, and the reaction mixture was stirred at 80 °C. The mixture was then purified by chromatography using a SCX cartridge to give the title compound as a yellow oil. ^{1}H NMR, $CDCl_3$: δ ppm 1.08−1.14 (m, 1 H), 1.49 (d, 1 H), 1.51−1.57 (m, 1 H), 1.65−1.71 (m, 1 H), 1.95 (d, 1 H), 2.10 (dd, 1 H), 2.30−2.36 (m, 2 H), 2.63 (d, 1 H), 2.84−2.91 (m, 1 H), 3.35−3.41 (m, 1 H), 3.66 (dd, 1 H), 7.03 (dd, 1 H), 7.27 (overlapped with $CDCl_3$, 1 H) 7.33 (d, 1 H). MS (m/z): 268 $[MH]^+$.

The two enantiomers were separated by chiral HPLC: column, Chiralcel OD-H; mobile phase, *n*-hexane/ethanol + 0.1% isopropylamine 90/10% v/v; flow rate, 14 mL/min; UV, 230 nm.

The enantiomeric excess was verified using the following chromatographic conditions: column, Chiralcel OD-H; mobile phase, *n*-hexane/ethanol + 0.1% isopropylamine 90/10% v/v; flow rate, 1 mL/min; DAD, 210−340 nm; retention times, 8.34 and 9.49 min.

Acknowledgment. We thank all the colleagues who helped in generating the data reported in this manuscript, in particular A. Nalin, Dr. F. Ferroni, Dr. G. Tamborrino, and Dr. Doug Minick. We also thank Dr. D. Donati, Dr. J. Hagan, and Dr. T. Rossi for their support during the program life. Finally we thank Dr. C. P. Leslie for careful proofreading of the manuscript.

References

(1) (a) Kulkarni, S. K.; Dhir, A. Current investigational drugs for major depression. *Expert Opin. Invest. Drugs* **2009**, *18*, 767–788. (b) Wong, M. L.; Licinio, J. From monoamines to genomic targets: a paradigm shift for drug discovery in depression. *Nat. Rev. Drug Discovery* **2004**, *3*, 136–151. (c) Millan, M. J. The role of monoamines in the actions of established and "novel" antidepressant agents: a critical review. *Eur. J. Pharmacol.* **2004**, *500*, 371–384. (d) Nemeroff, C. B. The burden of severe depression: a review of diagnostic challenges and treatment alternatives. *J. Psychiatr. Res.* **2007**, *41*, 189–206.

(2) (a) Arnt, J.; Christensen, A. V.; Hyttel, J. Pharmacology in vivo of the phenylindan derivative, Lu-19,005, a new potent inhibitor of dopamine, noradrenaline and 5-hydroxytryptamine uptake in rat brain. *Arch. Pharmacol.* **1985**, *329*, 101–107. (b) Chen, Z.; Skolnick, P. Triple uptake inhibitors: therapeutic potential in depression and beyond. *Expert Opin. Invest. Drugs* **2007**, *16*, 1365–1377. (c) Rakofsky, J. J.; Holtzheimer, P. E.; Nemeroff, C. B. Emerging targets for antidepressant therapies. *Curr. Opin. Chem. Biol.* **2009**, *13*, 291–302. (d) Liang, Y.; Shaw, A. M.; Boules, M.; Briody, S.; Robinson, J.; Oliveros, A.; Blazar, E.; Williams, K.; Zhang, Y.; Carlier, P. R.; et al. Antidepressant like pharmacological profile of a novel triple reuptake inhibitor, (1S,2S)-3-(methylamino)-2-(naphthalen-2-yl)-1-phenylpropan-1-ol (PRC200-SS). *J. Pharmacol. Exp. Ther.* **2008**, *327*, 573–583. (e) Skolnick, P.; Popik, P.; Janowsky, A.; Beer, B.; Lippa, A. S. "Broad spectrum" antidepressants: is more better for the treatment of depression? *Life Sci.* **2003**, *73*, 3175–3179. (f) Aluisio, L.; Lord, B.; Barbier, A. J.; Fraser, I. C.; Wilson, S. J.; Boggs, J.; Dvorak, L. K.; Letavic, M. A.; Maryanoff, B. E.; Carruthers, N. I. In-vitro and in-vivo characterization of JNJ-7925476, a novel triple monoamine uptake inhibitor. *Eur. J. Pharmacol.* **2008**, *587*, 141–146. (g) Bannwart, L. M.; Carter, D. S.; Cai, H. Y.; Choy, J. C.; Greenhouse, R.; Jaime-Figueroa, S.; Iyer, P. S.; Lin, C. J.; Lee, E. K.; Lucas, M. C. Novel 3,3-disubstituted pyrrolidines as selective triple serotonin/norepinephrine/dopamine reuptake inhibitors. *Bioorg. Med. Chem. Lett.* **2008**, *18*, 6062–6066. (h) Papakostas, G. I. Dopaminergic-based pharmacotherapies for depression. *Eur. Neuropsychopharmacol.* **2006**, *16*, 391–402. (i) Skolnick, P.; Popik, P.; Janowsky, A.; Beer, B.; Lippa, A. S. Antidepressant-like actions of DOV21,947: a "triple" reuptake inhibitor. *Eur. J. Pharmacol.* **2003**, *461*, 99–104.

(3) Micheli, F.; Cavanni, P.; Arban, R.; Benedetti, R.; Bertani, B.; Bettati, M.; Bettelini, L.; Bonanomi, G.; Braggio, S.; Checchia, A.; Davalli, S.; Di Fabio, R.; Fazzolari, E.; Fontana, S.; Marchioro, C.; Minick, D.; Negri, M.; Oliosi, B.; Read, K. D.; Sartori, I.; Tedesco, G.; Tarsi, L.; Terreni, S.; Visentini, F.; Zocchi, A.; Zonzini, L. 1-(Aryl)-6-[alkoxyalkyl]-3-azabicyclo[3.1.0]hexanes and 6-(aryl)-6-[alkoxyalkyl]-3-azabicyclo[3.1.0]hexanes: a new series of potent and selective triple reuptake inhibitors. *J. Med. Chem.* **2010**, *53*, 2534–2551.

(4) Bettati, M.; Cavanni, P.; Di Fabio, R.; Oliosi, B.; Perini, O.; Scheid, G.; Tedesco, G.; Zonzini, L.; Micheli, F. Oxa-azaspiro derivatives: a novel class of triple re-uptake inhibitors. *ChemMedChem* **2010**, *5*, 361–366.

(5) Mamane, V.; Gress, T.; Krause, H.; Fuerstner, A. Platinum- and gold-catalyzed cycloisomerization reactions of hydroxylated enynes. *J. Am. Chem. Soc.* **2004**, *126*, 8654–8655.

(6) Bertani, B.; Di Fabio, R.; Micheli, F.; Tedesco, G.; Terreni, S. Preparation of Aza-Bicyclic Compounds as Inhibitors of Mono-Amines Re-Uptake and Antidepressant Agents. WO2008031772, 2008.

(7) Di Fabio, R.; Micheli, F.; Tedesco, G.; Terreni, S. Preparation of 3-Azabicyclo[4.1.0]heptanes as Therapeutic Monoamine Reuptake Inhibitors. WO2008031771, 2008.

(8) Cerep: Le Bois l'Evêque, 86600 Celle l'Evescault, France. www.cerep.fr.

(9) All the studies involving animals were carried out in accordance with European Directive 86/609/EEC governing animal welfare and protection, which is acknowledged by Italian Legislative Decree No. 116, January 27, 1992, and according to an internal review performed by the GlaxoSmithKline Committee on Animal Research and Ethics (CARE) and to the Company Policy on the Care and Use of Laboratory Animals.

(10) Burchall, C. J.; Soroko, F. E.; Rigdon, G. C. Potentiation of the behavioral effects of 5-hydroxytryptophan by BW 1370U87, a selective monoamine oxidase-A inhibitor. *Drug Dev. Res.* **1992**, *25*, 209–213.

(11) Bourin, M.; Chenu, F.; Prica, C.; Hascoet, M. Augmentation effect of combination therapy of aripiprazole and antidepressants on forced swimming test in mice. *Psychopharmacology* (*Heidelberg, Germany*) **2009**, *206*, 97–107.